ChemComm

Cite this: *Chem. Commun.*, 2012, **48**, 5097–5099

www.rsc.org/chemcomm

COMMUNICATION

A quantum dot-intercalating dye dual-donor FRET based biosensor†

Haiyan Zhang and Dejian Zhou*

Received 18th January 2012, Accepted 7th March 2012
DOI: 10.1039/c2cc30422h

We report herein the development of a novel quantum dot-intercalating dye dual-donor FRET system that can be used for sensitive detection of pM level DNA and protein targets.

Quantum dots (QDs) have unique, size-dependent optical and electrical properties that can be exploited in a range of sensing, biomedical, and material applications.[1] Their broad absorption and narrow, symmetric emission are particularly well-suited for Förster resonance energy transfer (FRET) based sensing applications, because such spectral characteristics enable the wide selection of excitation wavelengths to minimise direct excitation of the acceptor, reducing background and improving sensitivity. QD-FRET based sensors have shown great promise in biological and environmental sensing.[2–5] Despite these, the strict requirement of small donor–acceptor distance (r) for high FRET efficiency (E, hence high sensitivity) has posed a considerable challenge due to the significant size of the QD (core plus surface coating), which can be comparable or even greater than the Förster radius (R_0) of typical QD-dye FRET pairs prior to bioconjugation.[2] This is especially pronounced for commercial water-soluble QDs, whose hydrodynamic radii are typically 7.5–15 nm, greater than the R_0 of most QD-dye FRET pairs (*e.g.* 4–7 nm).[2] As a result, most QD-FRET sensors have relied on increasing the number of acceptors on each QD (n) to achieve high FRET efficiency,[4] because $E = nR_0^6/(r^6 + nR_0^6)$ in single-donor–multi-acceptor FRET systems (n = number of acceptors). Such systems, however, are inefficient for low target : QD ratio situations (*e.g.* 1 : 1).[4] To date, all QD-FRET sensors reported have used the QD as the sole energy donor (Fig. 1A),[2–5] which may not be optimum for high sensitivity. We found previously that the preferential intercalation of ethidium bromide (EB) to duplex DNA can be exploited for label-free detection of the nM level of a DNA target.[5a] Herein, we report the development of the first QD–EB dual-donor FRET system, where both the QD and intercalated EBs can FRET to the dye acceptor, leading to significantly improved overall FRET efficiency for each target DNA binding (Fig. 1B). We show that this system can be exploited for detection of the specific pM level of DNA and protein targets by incorporating a specific aptamer sequence to QD–DNA conjugates.

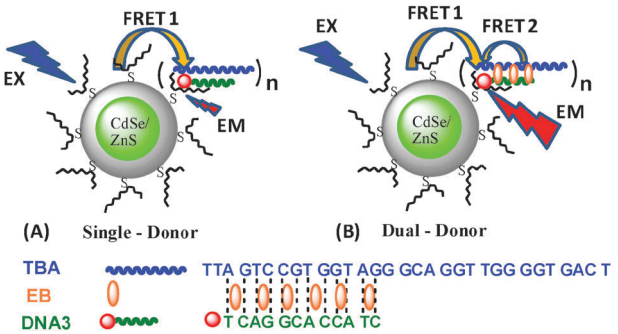

Fig. 1 Schematic comparison of the single-donor (A) and dual-donor (B) QD-FRET systems. The acceptor FRET signal comes from the energy transfer from the QD only (FRET1) in (A), but from both the QD (FRET1) and intercalated EBs (FRET2) in (B), leading to an enhanced overall FRET signal. The scheme beneath shows the DNA duplex sequences used herein.

In a conventional single-donor FRET system (Fig. 1A), the dye FRET signal comes from the energy transfer of the QD only, which is strongly dependent on the compactness of the QD–DNA conjugate; whereas in a dual-donor FRET system (Fig. 1B), both the QD and intercalated EBs FRET to the dye acceptor, leading to enhanced overall E. In addition, the spatial closeness of the intercalated EBs and acceptors[6a] in the dual-donor FRET system should enable efficient FRET even with relatively bulky QD–DNA conjugates (and/or a QD-dye FRET system with relatively small spectral overlap), bypassing the strict requirement of small r for efficient E in single-donor FRET systems. Furthermore, EB intercalates preferentially to double-stranded (ds) DNA with a 20-fold increase in fluorescence intensity,[6b] which should increase the E for each DNA target binding and hence sensitivity.

A glutathione (GSH) capped CdSe–ZnS core–shell QD (GSH–QD, $\lambda_{EM} \approx 540$ nm, crystal diameter ≈ 3.4 nm) was prepared by ligand exchange using our established procedures (see ESI†, Fig. S1).[5d] GSH binds to the QD mainly through coordination of its thiol group with the QD surface Zn^{2+} ion, leaving its two charged hydrophilic arms exposed to provide good water-solubility (see ESI†, Fig. S2). A target DNA (TBA, 5′ modified with a C_6-amine) containing a 29-mer anti-thrombin aptamer sequence[7] (shown in italic in Table 1) was covalently conjugated to the GSH–QD surface COOH group *via* EDC/NHS mediated coupling using our previous procedures.[5a] The average number of TBA attached to each QD was ~5 by measuring the difference between the amount of

School of Chemistry and Astbury Centre for Structural Molecular Biology, University of Leeds, Leeds LS2 9JT, UK.
E-mail: d.zhou@leeds.ac.uk; Fax: +44 (0)113 3436565; Tel: +44 (0)113 3436230

† Electronic supplementary information (ESI) available: Experimental details, supporting figures (chemical structure, TEM image and DNA and TB sensing spectra) and sensitivity comparison table. See DOI: 10.1039/c2cc30422h

Table 1 The DNA sequences and their abbreviations used in this study. TBA was modified with a $(CH_2)_6NH_2$ at 5′, and all other DNAs were labelled with Atto-647N at 3′

TBA	5′-TT*AGTCCGTGGTAGGGCAGGTTGGGGTGACT-3*′
DNA1	3′-TCAGGCACCATCCCGTCCAACCCCACTGA-5′
DNA2	3′-AATCAGGCACCATCC-5′
DNA3	3′-TCAGGCACCATC-5′
DNA3-SM	3′-TCAGACACCATC-5′
DNA-NC	3′-ATCGACCAACAT-5′

DNA used and that not conjugated to the QD (see ESI† for details),[5] denoted as QD–TBA_5 hereafter. Hybridization of complementary DNA3 (3′ labelled with an Atto-647N acceptor, Fig. 1) to the QD–TBA_5 will bring the acceptor in close proximity to the QD, producing QD to dye FRET as a readout signal.

Fluorescence spectra of QD–TBA_5 (40 nM) after hybridization with DNA3 (200 nM) excited at 450 nm (absorption minimum, λ_{min}, of Atto-647N to minimise direct dye excitation) revealed only a weak Atto-647N FRET signal at ~665 nm (Fig. 2A). This is presumably due to small spectral overlap between the QD emission and Atto-647N absorption (ESI†, Fig. S3), making QD to Atto-647N direct FRET inefficient (Atto-647N is not directly excited at 450 nm). When EB was introduced, the Atto-647N FRET signal was enhanced significantly (Fig. 2A). This agrees with that EB can intercalate the TBA–DNA3 duplex, acting as a second FRET donor for Atto-647N to increase the overall E (see ESI†, Fig. S4, for background corrected spectra). This is more clear from the plot of intensity ratio between the Atto-647N FRET signal (665 nm) and QD fluorescence (550 nm), I_{dye}/I_{QD}, *versus* EB concentration, [EB], which reveals a good positive linear relationship (R^2 = 0.976, Fig. 2B), confirming that addition of EB can indeed effectively increase the overall E of the system.

To investigate how target DNA length affects DNA sensing in this dual-donor QD FRET system, three complementary strands, DNA1 (29 mer), DNA2 (15 mer) and DNA3 (12 mer, Table 1) were hybridised to the QD–TBA_5 with 0.6 μM EB (to minimise EB contribution at dye emission). A plot of I_{Dye}/I_{QD} *versus* DNA

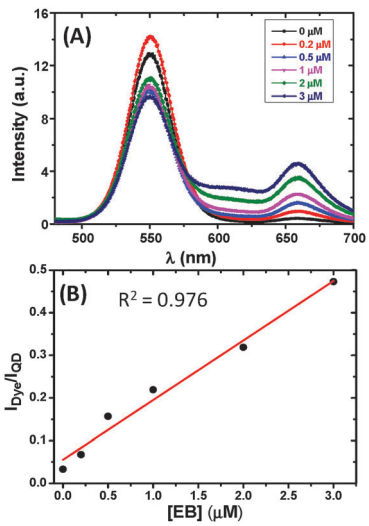

Fig. 2 (A) Fluorescence spectra of QD–TBA_5 (40 nM) after hybridization with DNA3 (200 nM) with different amounts of EB. The QD, EB, and Atto-647N fluorescence peak at ~550, 620 and 665 nm, respectively. (B) A plot of the Atto-647N to QD fluorescence intensity ratio, I_{Dye}/I_{QD}, as a function of [EB], the data were fitted to a linear function.

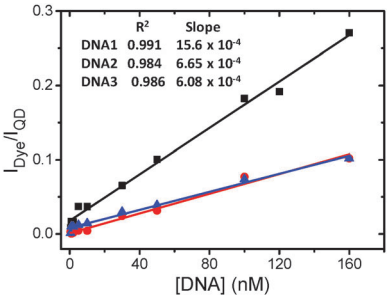

Fig. 3 A I_{Dye}/I_{QD} *vs.* [DNA] plot for three different DNA probes, all data were fitted to linear function.

concentration is shown in Fig. 3 (see ESI†, Fig. S5, for their [EB + ssDNA] background corrected fluorescence spectra). Although ssDNAs with certain local folding segments have been reported to bind to EB,[6c] the ssDNAs used here showed minimum binding.

Fig. 3 clearly shows that the I_{Dye}/I_{QD} increases linearly with the increasing DNA concentration (R^2 = 0.991, 0.984, and 0.986 for DNA1, DNA2, and DNA3, respectively) over the 0–160 nM range, suggesting that this system can be used to quantitate nM DNA targets. The detection limit here (~0.5 nM) is comparable or better than those of most other QD-FRET based DNA sensors and other established DNA sensors using direct detection (see ESI†, Table S1). The I_{Dye}/I_{QD} value showed a general trend of DNA1 > DNA2 > DNA3 under identical conditions. The rate of I_{Dye}/I_{QD} increase as a function of [DNA] also exhibited the same trend of DNA1 > DNA2 > DNA3 ($15.6 > 6.65 > 6.08 \times 10^{-4}$ nM^{-1}), which appears to be positively correlated with the length of the DNA target (29, 15 and 12 mer). Presumably because as the DNA target length increases, more EB molecules can be intercalated to each target DNA–TBA duplex, increasing the EB to Atto-647N FRET and hence the overall E.

To investigate the specificity of the dual-donor FRET sensor for DNA detection, DNA-NC (non-complementary) and DNA3-SM (single-base mismatch) were compared with DNA3 under identical conditions (with 0.6 μM EB). The resulting fluorescence spectra showed that DNA3 produced significantly stronger FRET than DNA3-SM, while DNA-NC produced the weakest signal. This is clearer after correction of the (EB + ssDNA) fluorescence background (see ESI†, Fig. S6), where DNA-NC produced almost no detectable FRET signal, suggesting that this sensor is specific and can discriminate between full-match and single-base mismatch targets, which is equivalent to a single-nucleotide polymorphism, SNP, discrimination. Despite a number of QD-FRET based DNA sensors reported in the literature, most have showed only limited discriminations between full- and non-matched DNAs (with discrimination ratios typically <3), few have demonstrated SNP discrimination ability, which is important for disease diagnosis (see ESI†, Table S1).[3–5]

We have further extended this dual-donor FRET sensor for label-free protein detection *via* the 29-mer anti-thrombin (TB) aptamer sequence incorporated in the TBA strand which has high affinity (K_d ≈ 0.5 nM) for TB.[7] The formation of a TBA–TB complex will detach the complementary DNA from the QD–TBA–DNAx conjugate, reducing the QD to Atto-647N (and also intercalated EBs) FRET, leading to QD fluorescence recovery.

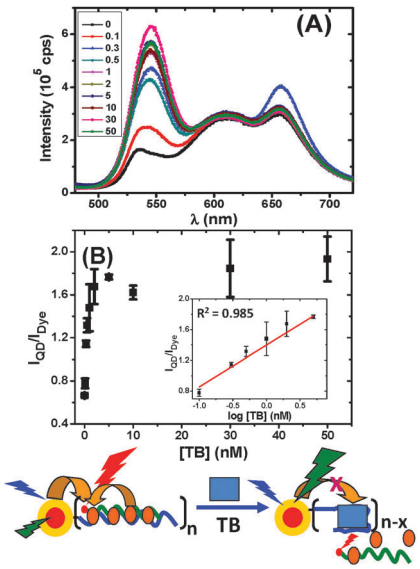

Fig. 4 (A) Fluorescence spectra of the dual-donor FRET sensor with different [TB] (nM). (B) A plot of the I_{QD}/I_{Dye} as a function of [TB]. Inset: a plot of I_{QD}/I_{Dye} *versus* log[TB] over the 0.1–10 nM range fitted to a linear function. Error bars show standard deviation of two experiments.

The assay was performed by hybridising QD–TBA_4 (a 2nd batch, with each QD conjugated to 4 TBA strands) to 4 mole equivalents of DNA2 in PBS (with 0.6 μM EB) for 2 h, followed by addition of different amounts of TB for 0.5 h before the fluorescence spectra were recorded. DNA2 was used here because it is shorter than the anti-TB aptamer sequence (15 *vs.* 29 mer), ensuring that TB binding can effectively displace it from the TBA–DNA2 duplex. Since FRET only happens over short distances (*ca.* <10 nm), any unbound species cannot participate in FRET and are hence undetected, allowing the assay to be carried out in a convenient, separation-free format.[3–5]

The QD fluorescence (~550 nm) was enhanced significantly as TB was introduced (Fig. 4A), which agrees well with that the formation of an aptamer–TB complex would detach a DNA2 from the QD–TBA_4 conjugate, reducing QD to dye (and EB) FRET, and leading to QD fluorescence recovery. 100 pM TB produced a significant enhancement of the QD fluorescence (see Fig. 4A), suggesting that this sensor has a detection limit of ~30 pM for TB, 2–4 orders of magnitude lower than that of previous single-donor QD-FRET sensors for TB.[4b,5c] In fact, this is one of the most sensitive label-free QD-aptamer FRET based sensors for protein detection using conventional fluorescence spectroscopy.[3–5] Its sensitivity is also comparable to those of some recently reported sensitive electrochemical sensors for TB detection.[8] An advantage of this sensor here is its ratiometric signal, which is effectively insensitive to instrumental noise or signal fluctuation, allowing for accurate, reliable detection.[2,5] The I_{QD}/I_{Dye} ratio increased linearly (R^2 = 0.985) with the log[TB] over the 0.1–10 nM range, suggesting that it can be used to quantitate pM level TB. We noticed that the Atto-647N signal did not change much as TB was added, despite a significant increase of the QD fluorescence, possibly due to not all TBAs on the QD surface being accessible for TB binding. This observation is similar to an earlier report of a QD–DNA molecular beacon based DNA sensor, where target DNA hybridization produced a significant increase of QD fluorescence but almost no change of the acceptor dye FRET signal.[3j] Replacing DNA2 (15 mer) with the shorter DNA3 (12 mer) in this dual-donor QD-FRET sensor led to a slightly lower sensitivity for TB (see ESI†, Fig. S7).

In summary, we have developed the first QD–EB dual-donor FRET system where both the QD and intercalated EBs can FRET to the dye acceptor, leading to significantly improved *E* for each DNA target binding. This sensor can detect sub-nM level labelled DNA with SNP discrimination ability. By incorporating the anti-TB DNA aptamer sequence, we have turned it into a sensitive, label-free protein sensor that can be used to quantitate the pM level of TB, 2–4 orders of magnitude more sensitive than those of single-donor QD-FRET based protein sensors.[2–5] Extension of this sensor to other DNA/RNA aptamers[9] may allow the development of a general, sensitive QD-FRET based sensing platform with broad applications in biosensing, environmental monitoring and disease diagnosis. Currently, we are focused on further optimising the QD surface and bioconjugation chemistries to make the sensor more robust and extend its application to real clinical samples.

We thank the Food and Environment Research Agency (FERA), the Leeds Biomedical Health Research Centre and the University of Leeds for funding this project.

Notes and references

1 (*a*) P. Alivisatos, *Nat. Biotechnol.*, 2004, **22**, 47; (*b*) X. Michalet, F. F. Pinaud, L. A. Bentolila, J. M. Tsay, S. Doose, J. J. Li, G. Sundaresan, A. M. Wu, S. S. Gambhir and S. Weiss, *Science*, 2005, **307**, 538.
2 I. L. Medintz and H. Mattoussi, *Phys. Chem. Chem. Phys.*, 2009, **11**, 17.
3 (*a*) T. Pons, I. L. Medintz, X. Wang, D. S. English and H. Mattoussi, *J. Am. Chem. Soc.*, 2006, **128**, 15324; (*b*) D. J. Zhou, J. P. Piper, C. Abell, D. Klenerman, D.-J. Kang and L. M. Ying, *Chem. Commun.*, 2005, 4807; (*c*) K. Susumu, H. T. Uyeda, I. L. Medintz, P. Thomas, J. B. Delehanty and H. Mattoussi, *J. Am. Chem. Soc.*, 2007, **129**, 13987; (*d*) Q. Wang, Y. Liu, Y. Ke and H. Yan, *Angew. Chem., Int. Ed.*, 2008, **47**, 316; (*e*) H. Peng, L. Zhang, T. H. M. Kjallman, C. Soeller and J. Travas-Sejdic, *J. Am. Chem. Soc.*, 2007, **129**, 3048; (*f*) D. E. Prasuhn, J. B. Blanco-Canosa, G. J. Vora, J. B. Delehanty, K. Susumu, B. C. Mei, P. E. Dawson and I. L. Medintz, *ACS Nano*, 2010, **4**, 267; (*g*) W. R. Algar and U. J. Krull, *Anal. Chim. Acta*, 2007, **581**, 193; (*h*) J. Liu, J. H. Lee and Y. Lu, *Anal. Chem.*, 2007, **79**, 4120; (*i*) H. Yao, Y. Zhang, F. Xiao, Z. Xia and J. Rao, *Angew. Chem., Int. Ed.*, 2007, **46**, 4346; (*j*) I. L. Madintz, L. Berti, T. Pons, A. F. Grimes, D. S. English, A. Alessandrini, P. Facci and H. Mattoussi, *Nano Lett.*, 2007, **7**, 1741; (*k*) R. Freeman, T. Finder and I. Willner, *Angew. Chem., Int. Ed.*, 2009, **48**, 7818; (*l*) C.-W. Chi, Y.-H. Lao, Y.-S. Li and L.-C. Chen, *Biosens. Bioelectron.*, 2011, **26**, 3346.
4 (*a*) S. Hohng and T. Ha, *ChemPhysChem*, 2005, **6**, 956; (*b*) M. Levy, S. F. Cater and A. D. Ellington, *ChemBioChem*, 2005, **6**, 2163; (*c*) C. Y. Zhang, H. C. Yeh, M. T. Kuroki and T. H. Wang, *Nat. Mater.*, 2005, **4**, 826; (*d*) E. Oh, M. Y. Hong, D. Lee, S. H. Nam, H. C. Yoon and H. S. Kim, *J. Am. Chem. Soc.*, 2005, **127**, 3270.
5 (*a*) D. J. Zhou, L. M. Ying, X. Hong, E. A. Hall, C. Abell and D. Klenerman, *Langmuir*, 2008, **24**, 1659; (*b*) D. J. Zhou, Y. Li, E. A. H. Hall, C. Abell and D. Klenerman, *Nanoscale*, 2011, **3**, 201; (*c*) H. Y. Zhang, P. G. Stockley and D. J. Zhou, *Faraday Discuss.*, 2011, **149**, 319; (*d*) Y. Zhang, H. Y. Zhang, J. Hollins, M. E. Webb and D. J. Zhou, *Phys. Chem. Chem. Phys.*, 2011, **13**, 19427.
6 (*a*) A. L. Benvin, Y. Greeger, G. W. Fisher, B. Ballou, A. S. Waggoner and B. A. Armitage, *J. Am. Chem. Soc.*, 2007, **129**, 2025; (*b*) F. He, Y. Tang, M. Yu, F. Feng, L. An, H. Sun, S. Wang, Y. Li, D. Zhu and G. C. Bazan, *J. Am. Chem. Soc.*, 2006, **128**, 6764; (*c*) P. He, E. Z. Tucker, C. B. Gorman and L. He, *Anal. Methods*, 2011, **3**, 2463.
7 Y. Kim, Z. Cao and W. Tan, *Proc. Natl. Acad. Sci. U. S. A.*, 2008, **105**, 5664.
8 (*a*) M. Zhou and S. J. Dong, *Acc. Chem. Res.*, 2011, **44**, 1232; (*b*) M. Zhou, Y. Du, C. G. Chen, B. L. Li, D. Wen, S. J. Dong and E. K. Wang, *J. Am. Chem. Soc.*, 2010, **132**, 2172.
9 (*a*) D. H. J. Bunka and P. G. Stockley, *Nat. Rev. Microbiol.*, 2006, **4**, 588; (*b*) J. W. Liu, Z. H. Cao and Y. Lu, *Chem. Rev.*, 2009, **109**, 1948.